Comparative Thermodynamic Environmental and Economic Analyses of Combined Cycles Using Air and Supercritical CO$_2$ in the Bottoming Cycles for Power Generation by Gas Turbine Waste Heat Recovery

Faiza Brahimi [1,2,*]**, Baya Madani** [1,3] **and Messaouda Ghemmadi** [1,3]

[1] Département de Génie Mécanique, Faculté de Technologie, Université M'hamed Bougara, Boumerdes 35000, Algeria

[2] Laboratoire Dynamique des Moteurs et Vibro-acoustique, Université M'hamed Bougara, Boumerdes 35000, Algeria

[3] Laboratoire d'Energétique Mécanique et Matériaux, Université Mouloud Mammeri, Tizi-Ouzou 15000, Algeria

[*] Correspondence: f.brahimi@univ-boumerdes.dz

Abstract: This study aims to improve existing fossil gas turbine power plants by waste heat recovery. These power plants function with an air simple cycle (ASC) and are implemented where water resources are limited. Modeling and simulation of ASC and two advanced energy conversion systems are performed. They are the gas turbine–air bottoming cycle (GT-ABC) and gas turbine–supercritical carbon dioxide bottoming cycle (GT-sc-CO$_2$BC). The main intent is to assess the benefits of employing sc-CO$_2$ as a working fluid in a closed Brayton bottoming cycle compared to air, based on the energetic and exergetic performance and economic and environmental impact. Analyses of ASC, GT-ABC, and GT-sc-CO$_2$BC are performed for various topping gas turbine powers: large (plant 1); medium (plant 2); and low (plant 3). The results of the energetic and exergetic analyses indicate that there is a significant improvement in the output power (ranging from 22% to 25%); and energy and exergy efficiencies of GT-ABC and GT-sc-CO$_2$BC (up to 8% and 11%, respectively) compared to that of ASC. To provide better insight into the behavior of these technologies and achieve their better integration, we investigate the influence of varying the bottoming compressor pressure ratio, the ambient temperature, and the gas flow rate in the bottoming cycle. The results of the environmental and economic analyses show that the amount of CO$_2$ emissions in GT-sc-CO$_2$BC is reduced by 10% more than in GT ABC. The results also show that GT-ABC improves the NPV between 17.69% and 30% but GT-sc-CO$_2$BC improves it even more, between 25.79% and 33.30%.

Keywords: exhaust heat recovery; gas turbine improvement; combined cycle; air bottoming cycle; supercritical carbon dioxide bottoming cycle

1. Introduction

With the increase in population all over the world and the development of countries, energy demand is constantly growing [1,2]. To satisfy the growing energy needs, production must be increased by establishing new installations or by improving existing ones. Gas turbines are widely used in thermal power generation units [3,4]. One alternative to improve a gas turbine is waste heat recovery (WHR), which has become an attractive research subject [5–7]. In the past decade, research on gas turbine WHR has achieved rapid progress, and several technologies have been developed [8], such as the gas–steam combined cycle (GSCC) using water or other alternative fluids [9,10]. Moreover, the organic Rankine cycle (ORC) is broadly used to generate power from low- and moderate-temperature heat sources [6,11–13]. RC and ORC are still limited because of the exergy destruction increase during the heating process, where the pure fluid evaporation takes

place at a constant temperature. This limitation has been circumvented by using binary fluids in the Kalina cycle and supercritical cycle where the heating process occurs at a variable temperature [14–16]. Compared to RC and ORC, the efficiency and power of the supercritical cycle were high and its cost was low [17]. The outstanding supercritical CO_2 (sc-CO_2) characteristics have motivated a high number of researchers used sc-CO_2 and have given enlightenments about the advantages of sc-CO_2 with different heat sources, industrial and mobile waste heat, geothermal heat, and solar energy [18–20]. In the late 1980s, the air bottoming cycle (ABC) was suggested to recover gas turbine waste heat (GT-ABC). It has been used in several applications [21,22]; it has had interesting performances compared to the gas turbine cycle alone. GT-ABC has been proposed by many studies conducted by [23] in heat engineering, the gas transport and storage industry, and the carbon dioxide capture installation of a coal-fired power unit. In electricity generation, GT-ABC increased the energy efficiency of a low-power-output gas turbine by about 10% and about 11% when using an intercooler. For both cycles, the energy efficiency was sensitive to different parameters such as the bottoming compressor and expander isentropic efficiency, the bottoming compressor pressure ratio, the heat exchange pressure drops, and the flue gases' temperature. Based on thermodynamic and economic comparative analyses [3], it has been shown that GSCC was thermodynamically better than the GT-ABC, even with an intercooler, since the system energy efficiency improvement exceeded 13%. However, from an economic point of view, based only on the investment expenditure evaluation, both cycles (GT-ABC and GT-ABC with intercooler) were better as their investment expenditures were smaller than those of GSCC. Operating under part-load conditions corresponding to a reduction in fuel mass flow, GT-ABC provided a slightly higher power output and energy efficiency than those of a simple gas turbine [24]. ABC is still interesting; in a very recent study [25], ABC was integrated with gas and steam cycles forming a complex system. It used the exhaust gases of a medium-output (78.3 MW) gas turbine for electrical power generation, and the steam cycle was placed under ABC for hydrogen production. Based on energy and exergy analyses, the results showed that ABC integration with the gas cycle allowed for an energy and exergy efficiency enhancement of 10.8% and 11.5%, respectively. Moreover, the ABC exergy destruction was only 9.3% of the total exergy destruction of the complex system. Economically, ABC, compared to the air simple cycle, achieved a payback period decrease of 1.65 years, a net present value increase of USD 9.4×10^8, and an internal rate of return (IRR) index improvement of about 110%. Moreover, the environmental damage effectiveness factor was found to be reduced by 30%. Studies on various working fluid Brayton cycles were performed [26]; they concluded that the s-CO_2 Brayton cycle has higher efficiency compared to other gas Brayton cycles. An important number of studies focused on showing the sc-CO_2 cycle advantages for different applications and various heat sources [27–29] including low-grade waste heat recovery [30], hybrid fuel cell systems [31], concentrated solar systems [32,33] and nuclear reactors [25,27]. The sc-CO_2 cycle allows, simultaneously, for some problems of the Rankine steam and others of Brayton gas cycles to be avoided and for some of their advantages to be kept [27]. CO_2 has all reasons to be chosen: it is nonflammable, non-explosive, nontoxic, noncorrosive, and abundant in nature. Furthermore, CO_2 has a low negative impact on the environment, as its ozone-depleting potential (ODP) and its global warming potential (GWP) are very low [17,34]. Recently, a study concerning the WHR of a gas turbine was conducted to show the potential of different sc-CO_2 cycles as bottoming cycles [35,36]. Compared to GT-ABC, combined gas turbine–supercritical CO_2 power cycles (GT-sc-CO_2BCs) have remarkably improved system performance. According to the sc-CO_2 cycle configuration, the gain in energy and exergy efficiencies was 30.22% to 33.4% and 31.9% to 48.3%, respectively. Regarding the environmental aspect, GT-sc-CO_2BCs with larger savings of CO_2 emissions remain better. From analysis and comparison of various sc-CO_2 cycle layouts, it was expected that the optimal layout depended on the sc-CO_2 cycle application. Combined with a topping large-power gas turbine and in terms of the net work and energy efficiency, [9] reported that among seven sc-CO_2 layouts selected, the complex cascade sc-CO_2 Brayton cycle

was the only cycle having higher performances compared to the steam cycle. Based on the thermodynamic analysis and optimization, [35] found that the most suitable layout for exhaust heat recovery from a gas turbine that provides a power of 35.5 MW was the combined gas turbine preheating cycle. Further to an energetic analysis of nine different sc-CO_2 bottoming Brayton cycle configurations to WHR from a very-low-power gas turbine (5 MW) [37], a partial-heating bottoming cycle was selected as an appropriate option. The Sc-CO_2 power cycle has not only been receiving attention as one of the promising alternatives for a power conversion system for its interesting energy and exergy efficiencies and its small size, but also for its economic benefit. Through an economic analysis conducted by [38] on combining a coal-fired power plant with various sc-CO_2 Brayton power cycles, the levelized cost of electricity (LCOE) was evaluated by using the total revenue requirement (TRR) method. It was found that all the analyzed sc- CO_2 cycles lead to an LCOE decrease of 7.8 to 13.6% compared to the steam Rankine cycle.

In the light of the previous studies, air and sc-CO_2 bottoming cycles offer the possibility to provide an interesting performance improvement of Brayton cycles. No research has targeted the comparison of GT-ABC and GT-sc-CO_2BC performance in terms of the energetic and exergetic performance, the environmental impact and the economic benefit. It is also noticed that the previous studies have particularly involved gas turbines providing low power.

This study focuses on the waste heat recovery systems with a target to improve the performances of existing gas turbines with different ranges of net power. The main purpose is to search for thermodynamic processes and power conversion methods, which can be applied as a bottoming cycle to produce additional power from the waste heat.

The specificity of the work is to find the appropriate combined cycle for waste heat recovery, without the requirement of a water–steam cycle, that is suitable for sites where there is a lack of water, based on the energetic and exergetic performance, CO_2 emissions savings, and economical impact, for low-, medium-, and large-scale power production.

Therefore, three configurations depicting the existing air simple cycle and two combined cycles are investigated: the simple air cycle (SAC) (Figure 1a); GT-ABC, where the bottoming cycle is an open-air Brayton cycle (Figure 1b); and GT-sc-CO_2BC, where the sc-CO_2 closed cycle is used as the bottoming cycle (Figure 1c). The results of modeling SAC, GT-ABC, and GT-sc-CO_2 BC are presented. The output power and the energy and exergy efficiencies of individual systems are determined and compared to select the best combined cycle. Through a sensitivity analysis, cycle optimum key parameters, which provide the system maximum performances, are obtained. The effects of the bottoming cycle pressure ratio, the ambient temperature, and the mass flow rate on the performances are delineated. Besides energy and exergy analyses of the cycles, an environmental analysis is performed. The contribution of the proposed cycles for reducing CO_2 emissions is underlined to emphasize the clean power plants. Because of the total cost importance in selecting a new system [39] and to make the study comprehensive, an economic analysis is also conducted. Important economic factors, such as the net present value (NPV), the levelized cost of electricity (LCOE), the resulting payback period (PP), and the internal rate of return (IRR), are estimated. These are the factors that will show the benefits of investing in these cycles.
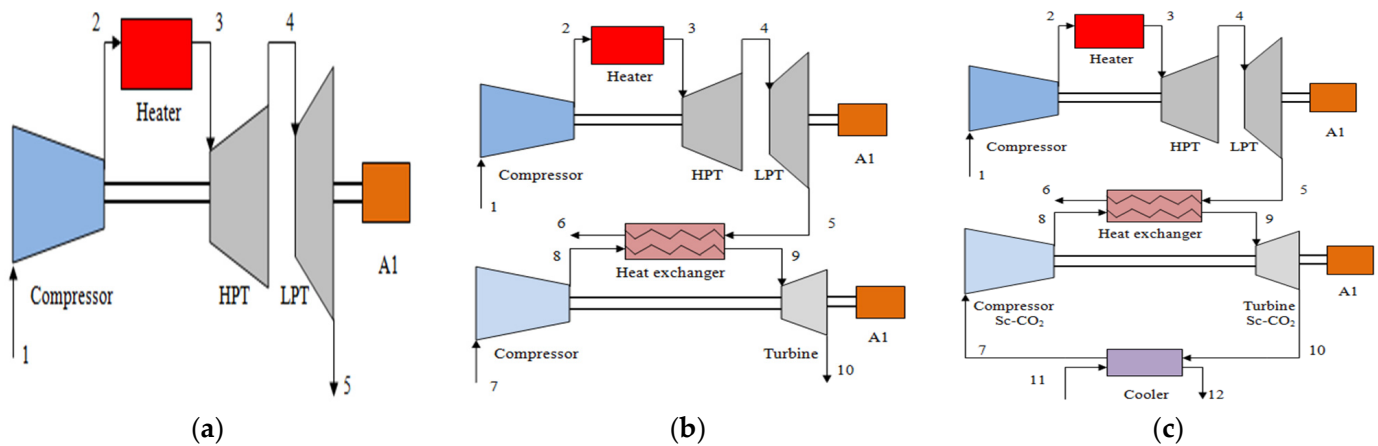
Figure 1. Layout of ASC (**a**), GT-ABC (**b**), and GT-sc-CO$_2$BC (**c**) 1, 2, 3, 4, 5, 6, 7, 8, 9, 10, 11 and 12 are the inlet and outlet of each component of the cycles.

2. Systems Description

Figure 1a shows the simple gas turbine, including a compressor, a combustion chamber, and a turbine. The installations considered are presented in Figure 1b,c; they refer to the combined cycles GT-ABC and GT-sc-CO$_2$BC. Gases exiting the topping turbine have considerably high temperature and mass flow rates. The bottoming cycles utilize these exhaust gases as a heat source in the heat exchanger for the bottoming compressor fluid before its admission to the bottoming turbine. Then, the heated fluid expands in the turbine, supplying additional power. Thermophysical and environmental characteristics of pure CO$_2$ and air are enclosed in Table 1.

Table 1. Important thermophysical and environmental properties of working fluids.

Working Fluid	Molar Mass (g/mol)	Pcr (Bars)	Tcr (°C)	Critical Density (g/cm^3)	Thermal Stability Limit (°C)	ODP	GWP	Auto Ignition Temperature (°C)	Flammability
Air	32	37.85	132.63	0.302	-	-	-	-	Not flammable
CO$_2$	44.01	73.8	30.95	0.469	800	0	1	N/A	Not flammable

As shown in (Figure 1b), in the case of GT-ABC, the air bottoming cycle is an open Brayton cycle. Air gets sucked up into the compressor at atmospheric conditions and discharged from the turbine at atmospheric pressure. However, in the case of GT-sc-CO$_2$BC (Figure 1c), the bottoming cycle is closed. After its expansion, sc-CO$_2$ is cooled down to the lowest cycle temperature in the cooler. The compressor inlet state is near the CO$_2$ critical point; in this region, the effects of real gas are significant, as shown by the low value of the compressibility factor, which decreases by 0.2–0.5, and the fluid becomes more incompressible and an important reduction in compression work can be achieved. Furthermore, near the critical point, the variation in pressure and temperature has a significant effect on the thermophysical properties of CO$_2$ [34,40]. Physical properties with the temperature of the sc-CO$_2$ are available in [34]. Unlike the steam Rankine cycle and air Brayton cycle where the minimum pressure in the system is about 0.07 MPa and 0.1 MPa, respectively, the sc-CO$_2$ cycle's minimum pressure is high; it corresponds to the CO$_2$ critical pressure. On the other hand, because of the piping and measurement system's capital cost, the maximum pressure cannot achieve high values. Hence, the pressure ratio will be low.

Since the performances of the combined cycle are closely dependent on the topping gas turbine outlet temperature, the exhaust temperature used is above 450 °C. The performance data at the standard conditions (15 °C and 1.013 bars) of the three plants used in this study are presented in Table 2. Tables 3–5 enclose the characteristics of the three cycles analyzed in this study.

Table 2. Performance specifications of the selected plants.

	Power (MW)	Efficiency (%)	Pressure Ratio	Exhaust Gases Mass Flow Rate (kg/s)	Exhaust Temperature (°C)
Plant 1	205.62	37.10	11	634.25	514
Plant 2	167.8	36	9.9	534.4	522
Plant 3	36.6	34.36	7.5	144.82	456

Table 3. Proprieties of ASC.

	Compressor Inlet Pressure (Bar)	Compressor Inlet Temperature (°C)	Pressure Ratio	Compressor Isentropic Efficiency (%)	Turbine Isentropic Efficiency (%)	Combustion Efficiency (%)	Fuel Mass Flow Rate (kg/s)	Air Mass Flow Rate (kg/s)	Maximal Turbine Inlet Temperature (°C)
Plant 1	1	25	11	0.85	0.88	0.96	13.25	621	1300
Plant 2	1	25	9.9	0.87	0.88	0.96	10	524.40	1100
Plant 3	1	25	7.5	0.87	0.88	0.93	2.39	142.43	1000

Table 4. Proprieties of ABC with optimal air mass flow rate.

	Compressor Inlet Pressure (Bar)	Compressor Inlet Temperature (°C)	Pressure Ratio	Compressor Isentropic Efficiency (%)	Turbine Isentropic Efficiency (%)	Air Mass Flow Rate (kg/s)
Plant 1	1	25	3.3	0.85	0.88	390
Plant 2	1	25	3	0.85	0.88	360
Plant 3	1	25	2.9	0.85	0.88	102

**Table 5.** Proprieties of sc-CO_2 BC.

	Compressor Inlet Pressure (Bar)	Compressor Inlet Temperature (°C)	Pressure Ratio	Compressor Isentropic Efficiency (%)	Turbine Isentropic Efficiency (%)	CO_2 Mass Flow Rate (kg/s)
Plant 1	74	31.25	3	0.85	0.88	390
Plant 2	74	31.25	3	0.85	0.88	360
Plant 3	74	31.25	3	0.85	0.88	102

3. Energetic and Exergetic Analyses

Figures 2 and 3 show the thermodynamic process in a temperature-entropy (T-s) diagram of an air simple cycle (ASC) and of a dual gas turbine combined cycle (GT-ABC and GT-sc-CO_2BC), respectively.
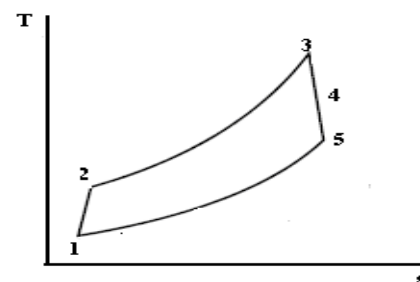
Figure 2. (T-s) diagram of air simple cycle (1, 2, 3, 4 and 5 are the inlet and outlet of each component of ASC in Figure 1a).
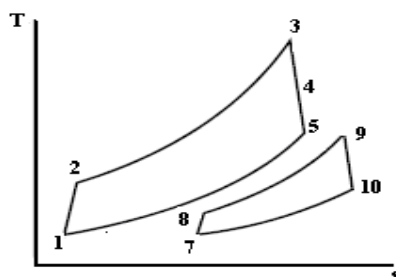
Figure 3. (T-s) diagram of the dual gas turbine combined cycle (1, 2, 3, 4, 5, 7, 8, 9 and 10 are the inlet and outlet of each component of GT-ABC and GT-sc-CO$_2$BC in Figure 1b,c).

Energy analysis is conducted for the three configurations (ASC, GT-ASC, and GT-sc-CO$_2$BC). The energy balance equations applied for each component of the topping and bottoming cycles are listed in Table 6.

Table 6. Model of energy analysis.

Cycle	Component	Model of the Energy Relation
Topping cycle	Compressor	$P_{TC} = \frac{1}{\eta_{is,c}}\left[\dot{m}_{air}Cp_{air}T_1\left(\pi_{air}^{\left(\frac{\gamma_{air}-1}{\gamma_{air}}\right)} - 1\right)\right]$
	Heater	$P_H = \dot{m}_f . PCI . \eta_H$
	Turbine	$P_{TT} = \eta_{is,T}.m_{eg}C_{Peg}T_3\left[1 - \left(\frac{1}{\pi_{air}}\right)^{\frac{\gamma_{eg}-1}{\gamma_{eg}}}\right]$
Bottoming cycle	Compressor	$P_{BC} = \frac{1}{\eta_{is,c}}\left[\dot{m}_{ig}Cp_{ig}T_{10}\left(\pi_{ig}^{\left(\frac{\gamma_{ig}-1}{\gamma_{ig}}\right)} - 1\right)\right]$
	Heat exchanger	$P_{HEX} = \dot{m}_{ig}c_{pig}\varepsilon_{HEX}(T_8 - T_7)$ $\varepsilon_{HEX} = \frac{T_8-T_7}{T_5-T_7}$
	Turbine	$P_{BT} = \eta_{is,T}.\left[m_{eg}C_{peg}\varepsilon_{HEX}(T_5 - T_7) + m_{ig}Cp_{ig}T_7\right]\left[1 - \left(\frac{1}{\pi_{ig}}\right)^{\frac{\gamma_{ig}-1}{\gamma_{ig}}}\right]$
	Cooler	$P_{Co} = \dot{m}_{ig}C_{pig}\varepsilon_{co}(T_9 - T_{10})$

The thermodynamic model establishment is based on some adopted assumptions, presented as follows:

- Flow system is considered in a steady-state.
- Turbines and compressors have given isentropic efficiencies.
- Pressure losses in the heat exchangers are ignored.
- Variations of kinetic and potential energies of the fluid in all cycle components are negligible.

Based on the first law of thermodynamics, energy efficiency is defined by Equation (1) for ASC and by Equation (2) for GT-ASC and GT-sc-CO$_2$BC.

$$\eta_{th,ASC} = \frac{P_{TT} - P_{TC}}{P_H} \tag{1}$$

$$\eta_{th} = \frac{(P_{TT} + P_{BT}) - (P_{TC} + P_{BC})}{P_H} \tag{2}$$

In a real process, irreversibility happens in its different components. To identify the location and magnitude of this irreversibility, exergy analysis is required. Exergy is a destroyed quantity resulting in entropy creation; it represents the maximum available work delivered by a power system. Compared to the energy analysis, the exergy analysis is a powerful tool that ensures a significant evaluation of the system's efficiency. General methods used in the exergy analysis and its application are available in various studies [8,41],

where its effectiveness is also confirmed. Exergy analysis of the three cycles is performed by analyzing all components of the cycles. The relative exergy destruction in each component is determined. Assuming the heat source and ambiance at a constant temperature, the exergy depending on the temperature and pressure of each cycle state point is given by Equation (3).

$$E_i = m_i[(h_i - h_0) - T_0(s_i - s_0)] \tag{3}$$

where the subscripts "0" and "*i*" refer, respectively, to the ambient condition and the point state.

The exergy balance equations applied for each component of the topping and bottoming cycles are listed in Table 7. Based on the second law of thermodynamics, cycle exergy efficiency is given by Equations (4) and (5) for ASC and the combined cycles, respectively.

$$\eta_{ex} = \frac{P_{TT} - P_{TC}}{E_{P_H}} \tag{4}$$

$$\eta_{ex} = \frac{(P_{TT} + P_{BT}) - (P_{TC} + P_{BC})}{E_{P_H}} \tag{5}$$

Table 7. Model of exergy analysis.

Cycle	Component	Model of the Exergy Destruction
Topping cycle	Compressor	$L_{TC} = m_{air}(E_1 - E_2) + P_{TC}$
	Heater	$L_H = m_{air}E_2 + m_f E_f - m_{eg}E_3$
	Turbine	$L_{TT} = m_{eg}(E_3 - E_5) - P_{TT}$
Bottoming cycle	Compressor	$L_{BC} = m_{ig}(E_{10} - E_7) + P_{BC}$
	Heat exchanger	$L_{IHX} = m_{ig}(E_7 - E_8) + m_{eg}(E_5 - E_6)$
	Turbine	$L_{BT} = m_{ig}(E_8 - E_9) - P_{BT}$
	Cooler	$L_{Co} = m_{ig}(E_9 - E_{10}) + m_{Cof}(E_{11} - E_{12})$

The exergetic approach assesses the deviation of the considered cycles from the theoretical Carnot cycle. Thus, the thermal efficiency of the considered cycles and Carnot cycle are linked through the exergy efficiency, as defined in Equation (6).

$$\eta_{th} = \eta_{ex}\eta_{Carnot} \tag{6}$$

with:

$$\eta_{Carnot} = 1 - \frac{T_c}{T_h} \tag{7}$$

where *Tc* and *Th* denote the temperatures of the heat sink and heat source, respectively.

The calculation procedure in the cycles' thermodynamic analysis is illustrated in the following steps: First, the input parameters of the topping and bottoming cycles are specified separately. The input parameters of the topping cycle are compressor inlet temperature and pressure, pressure ratio, turbine inlet maximal temperature, turbine and compressor isentropic efficiencies, combustor chamber efficiency, the airflow rate, and the fuel mass flow rate. The input parameters of the bottoming cycle are compressor inlet temperature and pressure, pressure ratio, turbine and compressor isentropic efficiencies, the effectiveness of the heat exchanger, the airflow rate in the case of the air bottoming cycle, and the sc-CO$_2$ flow rate in the case of the sc-CO$_2$ bottoming cycle. The operating parameters for the analysis of the three cycles are outlined in Tables 3–5. Then, using energy balance relations, all topping cycle state points are calculated. Furthermore, the air mass flow sucked in by the bottoming compressor is chosen as decision variable. Using the energy exchange relation in the heat exchanger and its effectiveness, the pressure value at the bottoming compressor outlet is varied. The procedure is repeated for different mass flow

values of the air. The optimal fluid flow rate is fixed when we achieve the maximum of the bottoming turbine power. Based on component energy balance relations of the bottoming compressor and turbine, all bottoming cycle state points are determined. Moreover, the enthalpies, entropies, and exergies at all cycles' states are calculated, and based on the first and second laws of thermodynamics on individual components, we calculate compressors' and turbines' powers, calorific power, heat recovered, and exergy destruction. At the end, cycles' output power and energy and exergy efficiencies are calculated.

4. Environmental Impact Analysis

Power plants generating electricity or driving machines are considered an important source of CO_2. Because of fossil fuel consumption, they emit a large amount of CO_2. To eliminate or reduce CO_2 emissions into the atmosphere, which are significant contributors to climate change, an extensive number of studies were performed [42–44]. Recently, technology development has concentrated on the means to have clean and safe power plants. The purpose of this part is first to underline the contribution of GT-ABC and GT-sc-CO_2BC in saving the earth's ecosystem by minimizing the polluting emissions in low-, medium-, and large-scale power production plants, then to select the more environmentally friendly cycle. The amount of reduction in CO_2 emissions, which is one of the deciding parameters, is evaluated by Equations (8) and (9) [35]. GT-sc-CO_2BC emissions are not expected to exceed those of GT-ABC, since its bottoming cycle is closed, and in a closed cycle there are no harmful emissions. Hence, we can already claim that GT-sc-CO_2BC will environmentally make more of a profit than GT-ABC.

$$M_{CO_2} = \alpha_{CO_2} . P_{botcycle} \qquad (8)$$

$$\alpha_{CO_2} = HR_{Ng} . EF_{Ng} \qquad (9)$$

where α_{CO_2} is the amount of CO_2 released from fossil fuel power plants for 1 kWh production. HRNg is the average operating heat rate and EFNg is the emission factor of natural gas.

5. Economic Analysis

An energetic system is not considered attractive for only its thermodynamic advantages but also for its expected contribution to the national economy. However, the previous energetic, exergetic and environmental analyses are sustained, with some considerations regarding the economic advantages of the proposed cycles. The efficiency and costs are always linked. This part aims to evaluate the economic feasibility of GT-ABC and GT-sc-CO_2BC in electricity generation and find out whether a cycle is cost-effective and provides economic benefits. The topping gas turbine costs can be found in published information and at manufacturers, while those of the bottoming cycle must be estimated from the costs of the different components constituting the cycle [21]. To evaluate the cost potential of new technology, economic analysis is considered important and difficult work, because in most cases, an expert opinion is very necessary to assess the system components' cost [17]. This analysis is performed with the help of many recent economic assessments that have been performed for power plants [38]. The economic models applied for the three cycles are based on the capital and operating expenditure evaluation. First, we adopted the equations detailed in [45] to evaluate the investment costs of the most important components according to their technical characteristics and thermodynamic parameters. Afterward, the costs were updated using the chemical equipment plant cost index (CEPCI) since they were calculated in USD in 1985. The cycles are proposed for existing power plants; the offsite costs, such as the costs of piping, instruments, and land, as well as the civil cost, have been excluded in this analysis. The net present value (NPV), the levelized cost of electricity (LCOE), the payback period (PP), and the internal rate of return (IRR) are the most often economic indicators used to take an investment decision. Moreover, NPV and IRR are the main factors for the project's acceptability. The NPV is obtained by subtracting the present values of the cycles' cost from their benefit streams. To have an economic advantage, the

NPV of the system must be positive; on the opposite, if NPV is negative the system will be economically disadvantaged, even if the power production is increased. The cost functions and economic indicators used in this paper are presented in Table 8. The values of CEPCI from 1985 to 2019 are listed in Table 9.

Table 8. Model of economic analysis.

	Cost and Indicator	Cost and Indicator Functions
Cost function	total capital of investment	$TC_{invest} = \left(1 + \sum TC_{equip}\right) \times k_{ind}$ TC_{equip}: equipment total cost k_{ind}: indirect cost factor
	capital cost according to economic situation in year 2019	$TC_{invest\ 2019} = TC_{invest\ 1985} \cdot \frac{CEPCI_{2019}}{CEPCI_{1985}}$
	annual cost of fuel supplied	$AC_{fuel} = \zeta.P_f.H$ ζ: unit cost of fuel P_f: rate of supply of energy in the fuel H: operation hours of a year
	annual cost of operation and maintenance	$AC_{O\ \&\ M} = f_k.AC_{invest\ 2019}$ F_k: operation, maintenance, and insurance cost factor
Economic indicators	net present value	$NPV = \sum\limits_{i=0}^{N} \left(P_{na,i} \times p_{el,i}\right) - \left(TC_{invest} + TC_{fuel} + TC_{O\&M}\right)$ N: economic life time $P_{na,i}$: annual net power during year i $p_{el,i}$: retail price of electricity during year i TC_{fuel}: total fuel cost $TC_{O\&M}$: total operating and maintenance cost
	levelized cost of electricity	$LCOE = \frac{AC_{invest}+AC_{fuel}+AC_{O\ \&\ M}}{P_{na}}$ AC_{invest}: investment annual cost P_{na}: annual net power
	payback period	$PP = \frac{TC_{invest}}{P_{na}.p_{el}-AC_{fuel}-AC_{O\ \&\ M}}$
	internal rate of return	$0 = \frac{\sum\limits_{i=0}^{N} TC_{invest,i}}{(1+IRR)^i}$

Table 9. CEPCI values [46].

Year	1985	1996	2001	2006	2014	2016	2017	2018	2019
CEPCI	325	382	382	499.6	586.77	541.7	567.5	603.1	619.2

The comparative analysis aims to select a profitable cycle providing maximum output power, maximum thermodynamic efficiencies, minimum CO_2 emissions, maximum net present value, minimum levelized cost of electricity, and minimum payback period.

6. Results and Discussion

6.1. Validation

The available data in the studies by [47] and in [22] were used to validate the model of the GT-ABC. Table 10 shows a comparison between the GT-ABC energy efficiency and the increase in the power output of the model with those of [22]. The shaft power and the efficiency at the nominal point of the GT10 gas turbine in [22] are 25 MW and 35.2%, respectively. The increase in power output was evaluated by comparing the power output of GT-ABC with that of ASC. The discrepancy between the two results is very weak (0.7%) for the energy efficiency and it is less than 12% for the increase in power output.

Table 10. Comparison of model results with those of [22].

	Energy Efficiency (%)	Increase in Power Output (%)
Present work	42.31	23.13
[22]	42.61	20.28

Table 11 presents the gain in energy efficiency with GT-ABC of the model compared with the one of [47] for the GE-F5 simple gas turbine. The topping and bottoming pressure ratio are considered 25 and 6, respectively. The gain in energy efficiency was calculated by comparing between the energy efficiencies of GT-ABC and ASC. The comparison was made for three values of ambient temperature. As the ambient temperature increased, the gain in energy efficiency decreased. The difference between the two results is less than 11.5%, which indicates a good agreement.

Table 11. Comparison of model results with those of [47].

	Gain in Energy Efficiency (%) of GT-ABC		
Ambient temperature (°C)	0	25	45
Present work	8	7.7	7.2
[47]	8	7.3	7

6.2. Energetic and Exergetic Analyses

Based on the energetic and exergetic models presented above, a computer program was developed in MATLAB 9.2 to model the three cycles (ASC, GT ABC, and GT s-CO$_2$ BC), evaluate their thermodynamic performances, and carry out a parametric analysis. Net output power and energy and exergy efficiencies were used to assess and compare performance cycles.

Thermodynamic performance simulations of ASC, GT-ABC, and GT-sc-CO$_2$BC were conducted, and the results for different conditions are presented. For each plant, the optimum air mass flow rate for which the net output power is maximum was determined (Table 4). To maintain the same size of the bottoming cycle in the two combined cycles, we used the same mass flow rate values in the ABC and sc-CO$_2$BC investigations. The thermodynamic parameters at the bottoming turbine inlet are also determined for the different plants with TG-ABC and TG-sc-CO$_2$BC (Table 12). Representative energy and exergy performance data for all plants with ASC, GT-ABC, and GT-sc-CO$_2$BC are given in Tables 13 and 14 and Figure 4. Thermodynamic analysis results indicate that for the three plants, GT-sc-CO$_2$ BC provides the maximum output power. With ASC, GT-ABC, and GT-sc-CO$_2$BC, the output powers are, respectively, 205.62, 235.1, and 248.73 MW for the first plant, 167.8, 195, and 209 MW for the second plant, and 36.6, 44.78, and 45.58 MW for the third plant (Table 13). This observation also holds for the energy and exergy efficiencies, since the energy and exergy inputs of all cycles are similar. GT-sc-CO$_2$BC energy efficiency for the three plants is determined to be 44.87%, 44.78%, and 42.8%, respectively. With GT-ABC and ASC, their energy efficiencies are, respectively, 42.42% and 37% for the first plant, 41.85% and 36% for the second plant, and 42.31%, and 34.36% for the third plant (Table 13). GT-sc-CO$_2$BC exergy efficiency for the three plants is determined to be 58.41%, 58.39%, and 58.58%, respectively. With GT-ABC and ASC, their exergy efficiencies are, respectively, 55.89%, and 48.30% for the first plant, 56.07%, and 46.92% for the second plant, and 57.91%, and 47.02% for the third plant (Table 13). For the low-power gas turbine (plant 3), the performances of GT-ABC and GT-sc-CO$_2$BC are higher than those of ASC, but they are much closer. Both implementations (GT-ABC and GT-sc-CO$_2$BC) add about 8 points to the ASC energy efficiency and 11 points to its exergy efficiency, as well as an output power rise of 22.34% to 25.24%. In the case of gas turbines with medium and large power (plants 1 and 2), we notice that the output powers' difference in GT-ABC and GT-sc-CO$_2$BC is larger. For the same resource, GT-sc-CO$_2$BC produces more power. With ABC, the output power is between 14.33 and 16.20% greater than that in the ASC, but with GT-sc-CO$_2$BC,

the power rise is between 21 and 24.55%. ASC energy and exergy efficiencies are improved, respectively, by about 5 to 6 and 7.6 to 9.2 points with GT-ABC, and by about 7.9 to 9 and 10.1 to 11.5 points with GT-sc-CO_2BC. For all plants, the net power and energy and exergy efficiencies of GT-sc-CO_2BC are higher than those of ASC and GT-ABC. Thus, it is obvious that GT-sc-CO_2 BC performs better. This is partially due to high values of enthalpy for sc-CO_2 at high pressure. In GT-ABC, air is compressed from the ambient pressure, but in GT-sc-CO_2BC, sc-CO_2 is compressed from critical pressure; for the same pressure ratio, this leads to a higher turbine inlet pressure. Moreover, when the pressure is higher than the critical pressure, sc-CO_2 specific heat becomes high for a greater temperature range. After being compressed, sc-CO_2 enters the heat exchanger with a high Cp, then it decreases rapidly along the heat exchanger until it reaches a small value on the other end of the heat exchanger. When sc-CO_2 flows through the heat exchanger, its temperature will increase rapidly due to the sharp decrease in its specific heat (Cp). Sc-CO_2 has a huge potential to recover the energy when it enters the heat exchanger. Consequently, the specific energy content of sc-CO_2 will be higher compared to air that does not have this characteristic of Cp variation. This proves the significant influence of sc-CO_2 thermophysical properties in the heat transfer process. Hence, the gas turbine will produce more power. It is also clear and straightforward that when using sc-CO_2 as a working fluid the compression work can be substantially decreased, because at its critical pressure sc-CO_2 behaves as a liquid then; unlike air in GT-ABC, it requires less compression work. Exergy analysis can be used for selecting the most suitable cycle and optimization of the cycle operation. It also allows for the determination of losses for the system components and the entire cycle. The minimization of losses allows the system to perform better, and consequently the output power is maximized. The results in Table 13 show that a large part of the input fuel exergy of the systems has been wasted in the cycle's components. For the first plant, the input fuel exergy waste is 220, 185.5, and 177.1 MW with ASC, GT-ABC, and GT-sc-CO_2BC, respectively, which represents 51.70%, 44.11%, and 41.59% of the input fuel exergy. For the second plant it is 189.8, 152.8, and 148.9 MW representing 53.08%, 43.93%, and 40.61% of the input fuel exergy, and for the third one, the input fuel exergy waste is 41.2, 32.54, and 32.22 MW, which represents 51.98%, 42.09%, and 41.42% of the input fuel exergy. We notice that for the three plants, the input fuel exergy waste is less with GT-sc-CO_2BC. This leads to better exergy efficiency of the system (Table 13). Table 14 gives the results of exergy analysis for the first plant components with the three cycles under the conditions mentioned in Table 2. It can be observed from this table that most exergy losses take place in the combustion chamber, which is mainly because of the high irreversible nature of the combustion process. The exergy destruction rate to total exergy destruction (%) determines the relative exergy destruction of a component; the combustion chamber has the highest level, which is equal to 86.9% of the total. It is also shown in Table 14 that irreversibilities in the turbine, the compressor, and the heat exchanger are also factors of exergy destruction; they are the results of the huge pressure difference in the compressor and the turbine, and the huge temperature difference in the heat exchanger. The gas turbine, the compressor, and the heat exchanger have the second, third, and fourth rank in exergy loss, respectively, whereas intercooler experiences the least exergy loss. Table 14 also shows that the exergy destruction rate in the bottoming cycle components (compressor, heat exchanger, and turbine) of GT-ABC is higher than that of GT-sc-CO_2BC.
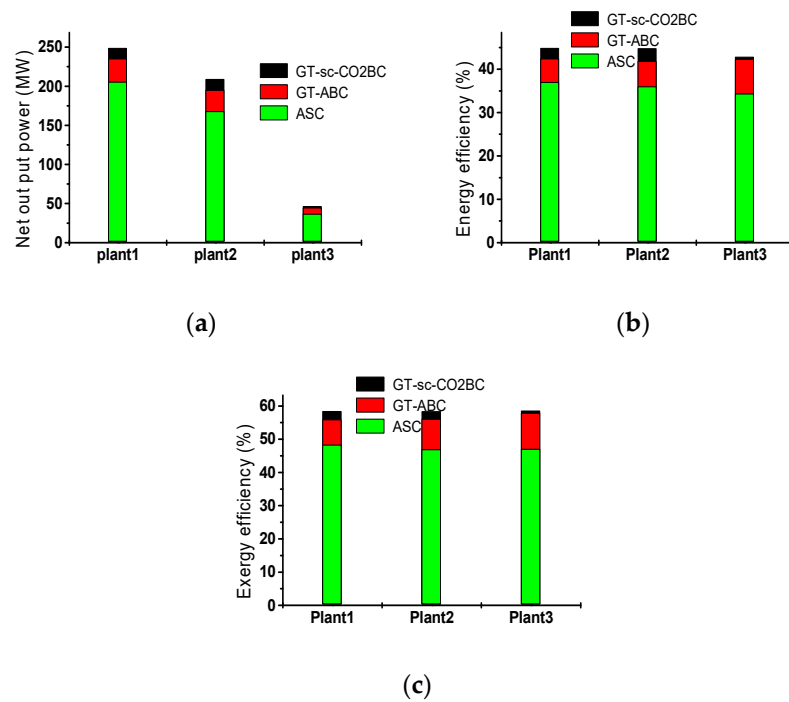
(**a**)

(**b**)

(**c**)

Figure 4. Net output power (**a**), energy efficiency (**b**), and exergy efficiency (**c**) for the different plants with the three cycles.

Table 12. Bottoming turbine inlet calculated pressure, temperature, and enthalpy for the different plants with TG-ABC and TG-sc-CO$_2$BC.

Plant	Plant 1		Plant 2		Plant 3	
Cycle	TG-ABC	TG-sc-CO$_2$BC	TG-ABC	TG-sc-CO$_2$BC	TG-ABC	TG-sc-CO$_2$BC
P (Bar)	3.3	222	3	222	2.9	222
T (°C)	379.45	458.58	374.11	350.19	332.37	307.88
H (kJ/kg)	694.61	1598.7	690.96	1500.5	637.02	1378.7

Table 13. Net output power, energy and exergy efficiencies, and exergy destruction for the different plants with the three cycles based on optimum pressure rate.

		Net Output Power (MW)	Energy Efficiency (%)	Exergy Destruction (MW)	Exergy Efficiency (%)
	ASC	205.62	37.10	220.10	48.30
Plant 1	TG-ABC	235.10	42.42	185.50	55.89
	TG-sc-CO$_2$BC	248.73	44.87	177.10	58.41
	ASC	167.80	36	189.80	46.92
Plan 2	TG-ABC	195	41.85	152.80	56.07
	TG-sc-CO$_2$BC	209.01	44.78	148.90	58.39
	ASC	36.60	34.36	41.20	47.02
Plant 3	TG-ABC	44.78	42.31	32.54	57.91
	TG-sc-CO$_2$BC	45.58	42.80	32.22	58.58

Table 14. Component exergy efficiency and exergy destruction rate to total exergy destruction with the three cycles for plant 1.

	Exergy Efficiency (%)			Exergy Destruction Rate to Total Exergy Destruction (%)		
	ASC	TG-ABC	TG-sc-CO_2BC	ASC	TG-ABC	TG-sc-CO_2BC
Air compressor	92.98	92.98	92.98	2.51	2.51	2.51
Combustion chamber	63.63	63.63	63.63	86.90	86.9	86.90
Gas turbine	97.08	97.08	97.08	3.77	3.77	3.77
Gas compressor	/	89.32	87.45	/	2.22	1.78
Heat exchanger	/	87.79	86.10	/	2.21	1.60
Gas turbine	/	98.56	94.01	/	2.37	2.03
intercooler	/	/	89.12	/	/	0.75
Cycle	48.30	55.89	58.41	/	/	/

6.3. Sensitivity Analysis

In this section, sensitivity analysis was carried out to evaluate the effects of various parameters on the thermodynamic results for the different cycles considered in this paper, including the effects of the bottoming compressor pressure ratio, ambient temperature, and gas flow rate in the bottoming cycle. These parameters are varied, while all others have the values given in Table 2. The thermodynamic performances of GT-ABC and GT-sc-CO_2BC were analyzed by varying the compressor pressure ratio at the limit of 1.5–8, the ambient temperature at the limit of 273–323 K, and the gas mass flow rate at the limit of 40–150 kg/s. When one specific parameter was studied, other parameters were kept constant. The simulations conducted are based on the heat exchanger and cooler efficiencies fixed to 85% and 75%, respectively.

A. Effect of the bottoming compressor pressure ratio

The range of the pressure ratio is set to 1.5–8, which is the pressure ratio range of the air bottoming cycle. It is noticed that the ASC performances are kept constant; they are not affected by the pressure ratio variation. Figure 5a, showing the net output power gain change of GT-ABC and GT-sc-CO_2BC with the pressure ratio, reveals that for each cycle, a maximum net output power can be achieved and the efficiency goes through a maximum value by increasing the pressure. In GT-ABC, the net output power gain increases firstly with increasing pressure ratio until its maximum, which is attained at an optimum pressure ratio. Afterward, it diminishes slightly, with the addition of the pressure ratio. This is mainly resulting from the sharp rise in power consumption in the compression process. As can be seen from Figure 5a, the optimum pressure ratio for GT-ABC is determined to be 3; it also yields to the maximum efficiencies of the cycle (Figure 5b,c). In GT-sc-CO_2BC, the observed behavioral trends are remarkable. They recorded a continuous increase in net output power and thermal and exergy efficiency gains. With a pressure ratio of 8, the gain can reach 15 MW in output power, 16% in energy efficiency, and 20.68% in exergy efficiency. The results may be clarified by analyzing the cycles' powers' evolution as well as the heat recovery process. Under the given values and assumptions as specified above, increasing the pressure ratio in ABC leads to an increase in both works of turbine and compressor (Figure 6a,b). Up to the optimum pressure ratio, the expansion work increase is higher than that of the compression, resulting in an advantageous effect on power and efficiencies. After this optimum point, the compressor work becomes dominant, leading to a decrease in power and efficiency. In sc-CO_2BC, it is clear that the powers of the compressor and turbine increase proportionally with the pressure ratio. However, the changes recorded between two pressure ratios show that the turbine power always increases significantly compared to the compressor power, as illustrated in Figure 6a,b. This behavior is related to the sc-CO_2 density, which remains big in the range of compressor exit temperature corresponding to the considered pressures. Figure 7 evaluates the energy amount in the heat exchanger recovered in ABC and sc-CO_2BC. For ABC, this energy amount is

related to the compressor inlet temperature, unlike sc-CO_2BC, where the compressor inlet temperature is always fixed at the CO_2 critical temperature. The net difference noticed in Figure 6 is due to sc-CO_2 specific heat, which is the main factor influencing the sc-CO_2 temperature profile in the heat exchanger. When the pressure ratio increases, the compressor outlet temperature will be higher and the necessary energy for fluids to achieve their heat exchanger outlet temperature will be less. This temperature is limited by the heat exchanger inlet temperature of exhaust gases. Consequently, the energy amount recovering for both fluids will decrease and the heat rest will be wasted in the atmosphere. Combining sc-CO_2BC with ASC, with the same compression ratio range, leads the initial output power of 36.6 MW to reach 51.6 MW; then, we obtain a gain of 15 MW. The thermal and exergy efficiencies, initially of 34.36% and 47.02%, can reach 50.36% and 67.70%, corresponding to an improvement of 16 and 21%. However, as was noticed before, the sc-CO_2 cycle is characterized by its low pressure ratio (around 2–3); the minimum pressure is limited by the critical pressure. However, the maximum pressure is also limited by the piping and measurement systems' capital cost. Despite this constraint, the maximum gain of the net output power, in this case, can achieve 10 MW, corresponding to thermal and exergy efficiency gains of 10% and 12.45%, respectively. In Figure 5a we notice a specific pressure rate for which the net output power gains provided by the two combined cycles are similar. However, in Figure 5b,c it is clear that the energy and exergy efficiencies of GT-sc-CO_2BC are always higher than those of GT-ASC, whatever the pressure rate. For the sc-CO_2 operating pressure rate limit, GT-sc-CO_2BC is rated better from the point of view of power and energy and exergy efficiencies.
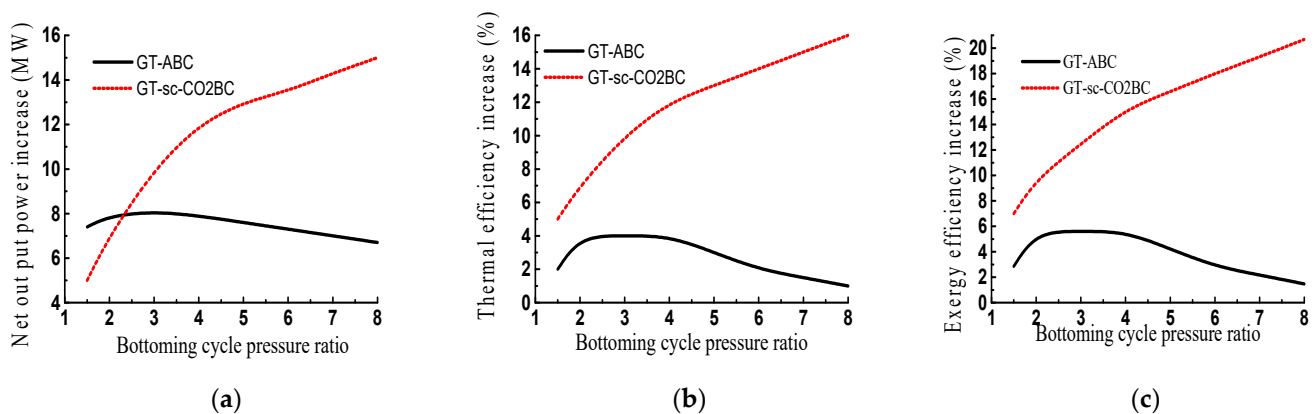

Figure 5. Net output power gain (**a**), thermal efficiency gain (**b**) and exergy efficiency gain (**c**) obtained with GT-ABC and GT-sc-CO_2BC compared with ASC versus pressure ratio (ambient temperature = 25 °C and gas mass flow rate = 390 kg/s).
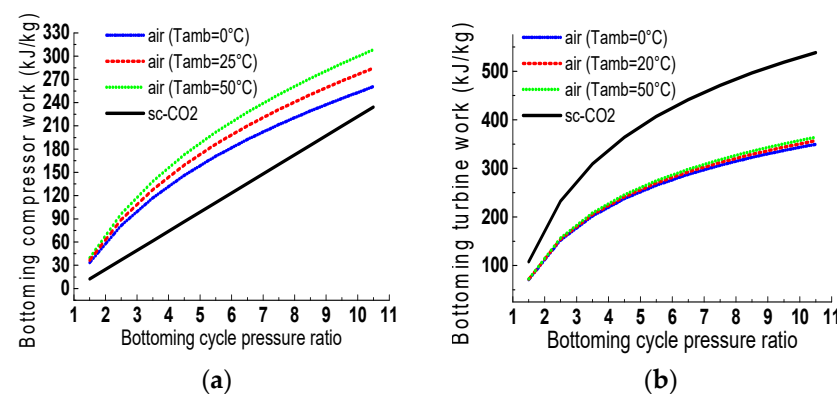

Figure 6. Bottoming compressor work (**a**) and turbine work (**b**) versus bottoming cycle pressure ratio with air at different ambient temperatures and with sc-CO_2.
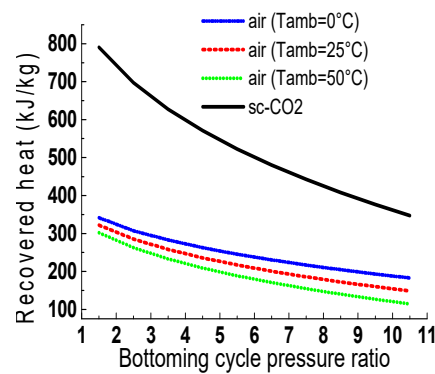
Figure 7. Recovered heat versus bottoming cycle pressure ratio with air at different ambient temperatures and with sc-CO_2.

B. Effect of the Ambient Temperature

The gas turbines can be used under hard climatic conditions. Far from the ISO standards, the ambient temperature varies considerably during the year; it can often reach over 50 °C involving an important reduction in its performance. Figure 8a–c show the sensitivity degrees of GT-ABC and GT-sc-CO_2BC net output power and energy and exergy efficiency gains, according to the ambient temperature which increases from 0 to 50 °C. Contrary to the previous case where ASC performances were not sensitive to changes in the parameters set out above, when the ambient temperature varies, ASC performances are directly affected because the inlet air of both topping and bottoming compressors is at atmospheric conditions. Unlike GT-ABC, where the net output power and energy and exergy efficiency gains decrease with the increase in ambient temperature, in GT-sc-CO_2BC, these performances increase. For an ambient temperature of 50 °C, there is a decline in GT-ABC output power gain (Figure 8a), resulting in a decrease in thermal and exergy efficiencies. In Figure 8a, it is noticed that for low temperatures less than 13 °C, the net output power gain difference between the two cycles is weak and their efficiencies are very close. However, it seems that improving an air simple cycle by GT-ABC is better. Since GT-ABC is made up of two compressors that draw in ambient air, at low temperature the air density is greater, which will allow for high power in topping and bottoming cycles. On the other hand, in GT-sc-CO_2BC, only the topping compressor sucks in ambient air.
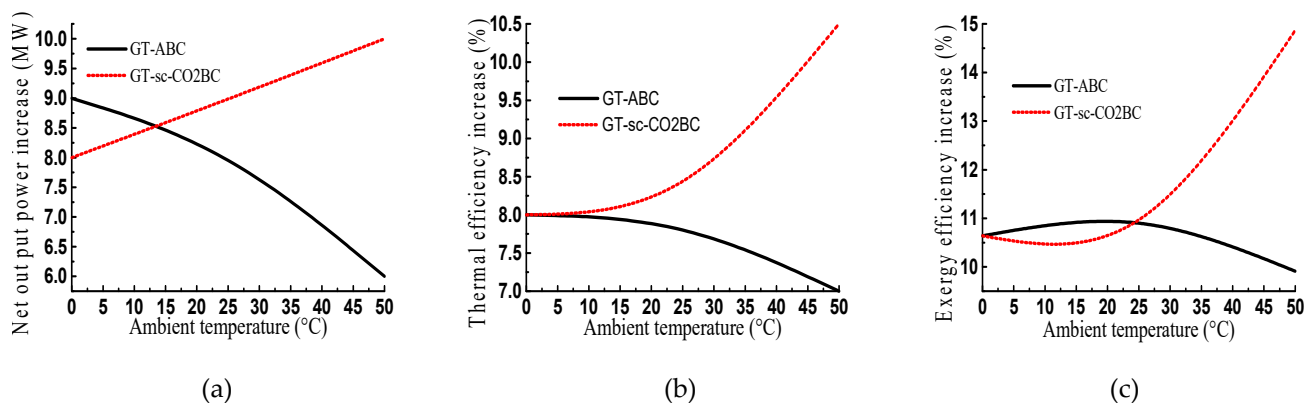

(a)   (b)   (c)

Figure 8. Net output power gain (**a**), thermal efficiency gain (**b**) and exergy efficiency gain (**c**) obtained with GT-ABC and GT-sc-CO_2BC compared with ASC versus ambient temperature (bottoming cycle pressure ratio = 3.3 and gas mass flow rate = 390 kg/s).

At 13 °C, GT-ABC and GT-sc-CO$_2$BC produce similar power, almost corresponding to the same thermodynamic efficiencies. For a temperature of more than 13 °C there is a sudden increase for GT-sc-CO$_2$BC and a decrease for GT-ABC in the net output power and thermodynamic efficiency gains. When the compressor inlet temperature is high, it is seen that GT-sc-CO$_2$BC performs relatively better. GT-ABC performance degradation is due to the decrease in air density in the topping and bottoming cycles simultaneously each time the inlet air temperature increases. Low density means a low mass flow rate, and this involves a less recovered heat amount in the heat exchanger (Figure 7).

For GT-sc-CO$_2$BC, the behavior is not similar because on one hand, the temperature change concerns only the topping flow rate; the sc-CO$_2$ flow rate is kept unchangeable. On the other hand, sc-CO$_2$ has a huge potential to recover the energy when it flows through the heat exchanger even in low-grade heat sources. It is shown that GT-sc-CO$_2$BC would have a thermodynamic benefit compared to GT-ABC, especially for high ambient temperatures. In contrast, for low temperatures, the GT-ABC performances are considered better.

C. Effect of gas mass flow rate

The two proposed cycles are investigated for the bottoming cycle gas flow rate change. The one of the topping cycle remains fixed. Figure 9a–c show the evolution of the net output power, thermal efficiency, and exergy efficiency gains, respectively, when the gas flow rate increases from 38 to 150 kg/s. It can be seen that GT-ABC and GT-sc-CO$_2$BC have different behaviors. Using GT-ABC, the net output power gain firstly rises to a maximum value (8.2 MW), and then it falls (Figure 9a). However, the energy and exergy efficiency gains continuously decrease from 8.1 to 6 and 11.22 to 8.34, respectively (Figure 9b,c). Moreover, up to a certain gas flow rate, the heat recovery allows for a high turbine inlet temperature and specific enthalpy, so the net power is improved. However, when the gas flow rate increases further, compressor consumption will be increased. Furthermore, the mean heat transfer temperature difference in the heat exchanger decreases, resulting in less enthalpy difference in the bottoming turbine. In this case, even if the mass flow is added, the net output power gain will decrease. As known, the energy efficiency is concerned with the net power output and calorific energy in the combustion chamber. As this last energy is not affected by the gas flow rate change, the comprehensive effect of the output power gain decrease results in efficiency gain reductions. However, the performance trend of GT-sc-CO$_2$BC depicted in Figure 9a–c is opposite to that of GT-ABC. This trend will promote the enhancement of its efficiencies and net output power gains. When increasing the gas flow rate, the net output power and energy and exergy efficiency gains keep rising from 2.9 MW to 10 MW, from 2.6% to 10% and from 3.68 to 13.83%, respectively. GT-sc-CO$_2$BC's advantage is the reduced compressor power, even if the sc-CO$_2$ flow rate increases. At 105 kg/s, both cycles produce similar output power; below this value, GT-ABC owns more output power gain, but above this value, it is GT-sc-CO$_2$BC that produces more. The gas flow rate corresponding to the same energy efficiency of both cycles is weaker (90 kg/s). Less than 90 kg/s higher energy efficiency gain is achieved with GT-ABC, but above 90 kg/s it is GT-sc-CO$_2$BC, which will provide higher energy efficiency gain. GT-sc-CO$_2$BC is advantageous because of its high performance for large working conditions, with a simple layout, compact turbomachinery, and heat exchanger. GT-sc-CO$_2$BC can be utilized to recover waste heat from low-, medium-, and large-power gas turbines to potentially improve the power and the energy and exergy efficiencies, which is less practically feasible with GT-ABC.
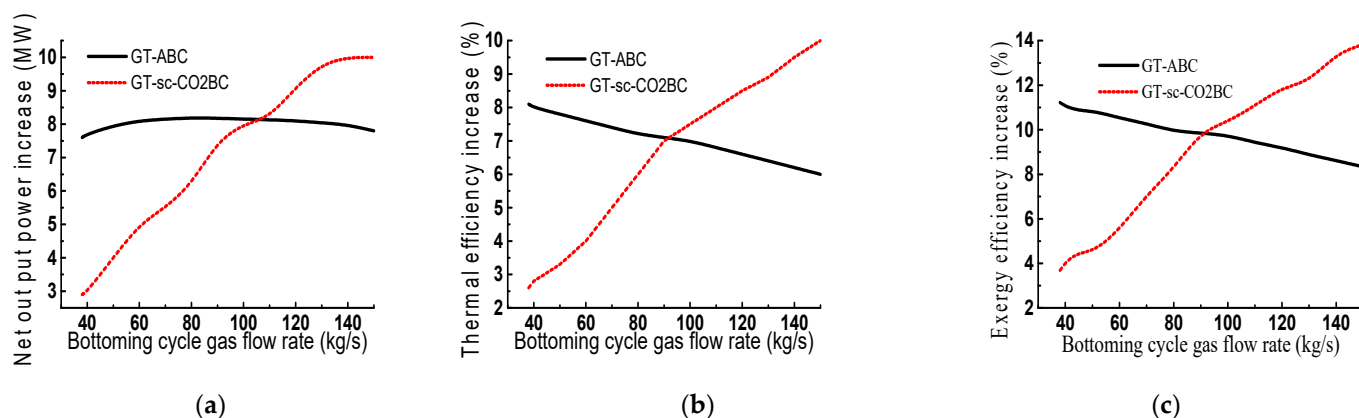
Figure 9. Net output power gain (**a**), thermal efficiency gain (**b**), and exergy efficiency (**c**) obtained with GT-ABC and GT-sc-CO$_2$BC compared with ASC versus gas flow rate (bottoming cycle pressure ratio = 3.3 and ambient temperature = 390 kg/s).

6.4. Environmental and Economic Analyses

This preliminary part provided interesting insights on the potential of GT-ABC and GT-sc-CO$_2$BC to reduce CO$_2$ emissions of a power generation process with ASC. The environmental benefits of GT-ABC and GT-sc-CO$_2$BC, compared with ASC having no emissions reduction, for the three plants are presented in Table 15. It shows that a significant CO$_2$ emission amount can be reduced by both cycles. However, the highest value of CO$_2$ emission reduction is that achieved by adopting an sc-CO$_2$ bottoming cycle. A comprehensive look at Table 15 shows that the CO$_2$ emission reduction in each cycle depends on the topping cycle power. For the low-scale power plant, the sc-CO$_2$ bottoming cycle can barely supply a 10% reduction relative to the air bottoming cycle. However, for medium- and large-scale power plants, the additional reduction is significant; it exceeds 50%. Based on these results, GT-sc-CO$_2$BC and GT-ABC with a larger reduction in CO$_2$ emissions are considered environmentally friendly cycles, but GT-sc-CO$_2$BC is the more favorable, whatever the plant power.

Table 15. CO$_2$ emission reduction for the different plants.

Plant	Cycle	MCO$_2$ (kg/h)
	TG-ABC	12,312.61
Plant 1	TG-sc-CO$_2$BC	18,005.32
	TG-ABC	11,360.35
Plant 2	TG-sc-CO$_2$BC	17,211.77
	TG-ABC	3416.46
Plant 3	TG-sc-CO$_2$BC	3750.60

In economic analysis, the NPV, LCOE, BP, and IRR are used as economic indicators to evaluate the benefits of investing in GT-ABC and GT-sc-CO$_2$BC. The economic performances for the individual cycles (ASC, GT-ABC, and GT-sc-CO$_2$BC) for the three plants shown in Table 16 are calculated, for a twenty-year operation period of 8000 operation hours per year, after converting the costs based on the current dollar standards. The results in Table 14 show that there is always a net positive profit, which means both cycles are attractive. ASC has a net current value smaller than those of GT-ABC and GT-sc-CO$_2$BC and for all plants combining the standalone gas turbine with air or sc-CO$_2$ bottoming cycle raises the NPV. The increase in the power output will obviously increase the plant revenue. However, this increase will partially be offset by the increase in capital cost associated with the installation and utility expenditures for the operation. The change in the economic performances of the cycles with the net power is shown in Table 16. As seen from this table, with the increase in the net power, the NPV of the cycles increases while

the LCOE decreases. Depending on the ASC output power, GT-ABC improves the NPV of ASC from 17.6% to 30%, and GT-sc-CO_2BC can improve it more from 25.79% to 33.30% (Figure 10). Moreover, it is illustrated that the LCOEs of GT-ABC and GT-sc-CO_2BC are slightly reduced as compared with that of ASC. This is mainly due to the plant size, where the number of cycle components in both combined cycles is reduced. It is also noticed that the NPV of GT-sc-CO_2BC is always higher than GT-ABC, and its corresponding LCOE is always lower than other LCOEs, indicating GT-sc-CO_2BC's ability to provide higher potential revenues. The LCOEs of GT-ABC and GT-sc-CO_2BC are very close, so these cycles are distinguished from ASC as the most economical plants in terms of the NPV. Consequently, the resulting payback period is between 2.54 and 5.2 years for ASC, while for GT-ABC and GT-sc-CO_2BC the payback period is between 2.77 and 5.3 years and 2.78 and 5.27 years, respectively. However, there is a significant difference in the payback period of a low-scale power plant compared with that of medium- and large-scale power plants, since the difference between the highest and the lowest values is more than 2,4 years. This confirms the strong link between the plant power and its payback period. It is noted that for the same plant, GT-ABC and GT-sc-CO_2BC can nearly maintain a similar ASC payback period. In consequence, it can be concluded that GT-ABC and GT-sc-CO_2BC can both be reasonable alternatives considering the payback period. IRR values of the different cycles are shown in Table 16. For all powers, the IRR index of ASC is about 36%, which slightly decreases in the case of GT-ABC and GT-sc-CO_2BC to about 34% and 33%, respectively. The diminution does not exceed 8%. Therefore, using GT-ABC and GT-sc-CO_2BC slightly affect the IRR, which substantiates the profitability of these cycles. It is evident that the net power generation dominates the economic performances of power plants. These results would make GT-ABC and GT-sc-CO_2BC economically interesting compared with ASC, and GT-sc-CO_2BC remains the most attractive and a good competitor for low-, medium-, and large-scale power generation.

Table 16. ASC, GT-ABC, and GT-sc-CO_2BC net present value for the three plants.

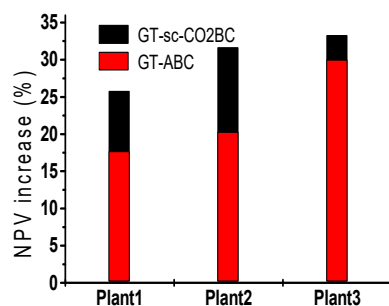|		NPV (M$)	NPV Increase (%)	LCOE ($/MWh)	PB (Year)	IRR (%)
	ASC	173.01		2.99	2.54	36.25
Plant 1	GT-ABC	203.63	17.69	2.83	2.77	34.38
	GT-sc-CO_2BC	217.64	25.79	2.75	2.78	33.44
	ASC	138.33		3.09	2.69	37.54
Plant 2	GT-ABC	166.40	20.29	2.91	2.94	35.35
	GT-sc-CO_2BC	182.12	31.65	2.80	2.92	34
	ASC	25.10		3.96	5.20	48.04
Plant 3	GT-ABC	32.63	30.00	3.69	5.30	44.78
	GT-sc-CO_2BC	33.46	33.30	3.66	5.27	44.37

Figure 10. NPV increase obtained with GT-ABC and GT-sc-CO_2BC compared with ASC.

7. Conclusions

This study illustrates the potential of an air bottoming cycle (ABC) and supercritical carbon dioxide bottoming cycle (sc-CO_2BC) in gas turbine waste heat recovery. In contrast

to the conventional combined cycle, these alternatives do not require bulky steam equipment. These cycles are suitable where water supply is limited or where there are weight and physical space restrictions.

Compared to the output power of a simple gas turbine (ASC), GT-ABC provides a greater output power of 14.33 to 16.20%, and with GT-sc-CO_2BC the output power increase is from 21 to 24.55%. Compared to the energetic performance of ASC, the improvement in the energy efficiency is from 5% to 8% in the case of GT-ABC, and from 7.9% to 9% in the case of GT-sc-CO_2BC. Compared to the exergetic performance of ASC, the improvement in exergy efficiency is from 7% to 11% in the case of GT-ABC, and from 10.1% to 11% in the case of GT-sc-CO_2BC. The thermodynamic performances of GT-sc-CO_2BC are better than those of GT ABC. According to the sensitivity analysis, the bottoming compressor pressure ratio, the ambient temperature, and the gas flow rate in the bottoming cycle are identified as factors affecting GT ABC and GT sc-CO_2BC performances. Compared to the CO_2 emissions of GT ABC, there is a 10% reduction in the amount of CO_2 emissions in the case of GT-sc-CO_2BC. The economic assessment expects a remarkable NPV improvement. With GT-ABC, the improvement in the NPV is from 17.69% to 30%, and with GT-sc-CO_2BC, it is from 25.79% to 33.30%. Concerning the payback period, GT-sc-CO_2BC and GT-ABC perform better for medium- and large-scale power plants since the payback period is below 3 years. Thus, GT-sc-CO_2BC is estimated to have promising economic potential for all levels of topping cycle power. Comparative analysis, based on the output power, the energy and exergy efficiencies, and environmental and economic benefits for lower-, medium-, and large-scale power plants, asserts that GT-sc-CO_2BC is the appropriate option and a promising technology for gas turbine waste heat recovery to produce additional power.

Furthermore, an experimental validation of this study will bring sufficient novelty to this research work. Further research is needed on various configurations to select the optimal layout for both air and sc-CO_2 cycles. Therefore, more comprehensive research studying other pure fluids or some new CO_2 mixtures in bottoming cycles is required.

More detailed modeling of the heat exchanger should be considered. For sites having water resources, a comparison with Rankine and organic Rankine cycles should be investigated. Furthermore, economic analysis can be enhanced by a sensitivity analysis to forecast the economic benefit changes.

Author Contributions: Conceptualization, F.B.; methodology, F.B.; software, M.G.; validation, M.G.; formal analysis, B.M.; resources, M.G.; writing—original draft preparation, F.B.; supervision, B.M. All authors have read and agreed to the published version of the manuscript.

Data Availability Statement: Not applicable.

Conflicts of Interest: The authors declare no conflict of interest.

Nomenclature

The following abbreviations, symbols, subscripts, and Greek letters are used in this manuscript:

		HEX	Heat exchanger
Symbols		ig	Inlet gas
Cp	Specific heat of fluid at constant pressure [J/kg·K]	is	Isentropic
E	Exergy [W]	n	Net out put power
m	Mass flow rate [kg/s]	T	Turbine
m_{fuel}	Fuel mass flow rate [kg/s]	TC	Topping compressor
P	Power [W]	TT	Topping turbine
LHV	Lower heating value [J/kg]	Abbreviations	
T	Temperature [K]	ASC	Air simple cycle

Subscripts		GT	Gas turbine
BC	Bottoming compressor	GT-ABC	Gas turbine–air bottoming cycle
BT	Bottoming turbine	GT-sc-CO_2 BC	Gas turbine–supercritical carbon dioxide bottoming cycle
C	Compressor	Greek letters	
Co	Cooler	π	Pressure ratio [-]
Cof	Cooling fluid	γ	Specific heats ratio [-]
eg	Exhaust gas	ε	Efficiency [%]
f	Fuel	η_{ex}	Exergy efficiency [%]
H	Heater	η_{th}	Energy efficiency [%]

References

1. Fengrui, S.; Yuedong, Y.; Mingqiang, C.; Xiangfang, L.; Lin, Z.; Ye, M. Performance analysis of superheated steam injection for heavy oil recovery and modelling of well bore heat efficiency. *Energy* **2017**, *125*, 795–804.
2. Pastor-Martinez, E.; Rubio-Maya, C.; Ambriz-Díaz, V.M.; Belman-Flores, J.M.; Pacheco-Ibarra, J.J. Energetic and exergetic performance comparison of different polygeneration arrangements utilizing geothermal energy in cascade. *Energy Convers. Manag.* **2018**, *168*, 252–269. [CrossRef]
3. Chmielniak, T.; Czaja, D.; Lepszy, S. Technical and economic analysis of the gas turbine air bottoming cycle. In Proceedings of the ASME Turbo Expo 2012 GT2012, Copenhagen, Denmark, 11–15 June 2012.
4. Yu, S.C.; Chen, L.; Zhao, Y.; Li, H.X.; Zhang, X.R. A brief review study of various thermodynamic cycles for high temperature power generation systems. *Energy Convers. Manag.* **2015**, *94*, 68–83. [CrossRef]
5. He, M.G.; Zhang, X.X.; Zeng, K.; Gao, K.A. A combined thermodynamic cycle used for waste heat recovery of internal combustion engine. *Energy* **2011**, *36*, 6821–6829. [CrossRef]
6. Zhu, S.; Deng, K.; Qu, S. Energy and exergy analyses of a bottoming Rankine cycle for engine exhaust heat recovery. *Energy* **2013**, *58*, 448–457. [CrossRef]
7. Zhang, L.; Pan, Z.; Zhang, Z.; Shang, L.; Wen, J.; Chen, S. Thermodynamic and Economic Analysis between Organic Rankine Cycle and Kalina Cycle for Waste Heat Recovery From Steam-Assisted Gravity Drainage Process in Oilfield. *J. Energy Resour. Technol.* **2018**, *140*, 122005. [CrossRef]
8. Saidur, R.; Rezaei, M.; Muzammil, W.K. Technologies to recover exhaust heat from internal combustion engines. *Renew. Sustain. Energy Rev.* **2012**, *16*, 5649–5659. [CrossRef]
9. Cho, S.K. Investigation of the bottoming cycle for high efficiency combined cycle gas turbine system with supercritical carbon dioxide power cycle. In Proceedings of the ASME Turbo Expo 2015, Turbine Technical Conference and Exposition GT2015, Montréal, QC, Canada, 15–19 June 2015.
10. Campos Rodriguez, C.E.; Escobar Palacio, J.C.; Venturini, O.J.; Silva Lora, E.E.; Cobas, V.M.; Marques dos Santos, D.; Lofrano Dotto, F.R.; Gialluca, V. Exergetic and economic comparison of ORC and Kalina cycle for low temperature enhanced geothermal system in Brazil. *Appl. Therm. Eng.* **2013**, *52*, 109–119. [CrossRef]
11. Vaja, I.; Gambarotta, A. Internal combustion engine (ICE) bottoming with organic Rankine cycles (ORCs). *Energy* **2010**, *35*, 1084–1093. [CrossRef]
12. Hugo, D.P. Working Fluid Dependence on Source Temperature for Organic Rankine Cycles. *J. Energy Resour. Technol.* **2020**, *142*, 012103. [CrossRef]
13. Chowdhury, M.; Mokheimer, E. Energy and Exergy Performance Comparative Analysis of a Solar-Driven Organic Rankine Cycle Using Different Organic Fluids. *J. Energy Resour. Technol.* **2021**, *143*, 102107. [CrossRef]
14. Knudsen, T.; Clausen, L.R.; Haglind, F.; Modi, A. Energy and exergy analysis of the Kalina cycle for use in concentrated solar power plants with direct steam generation. In Proceedings of the ISES Solar World Congress, Cancun, Mexico, 3–7 November 2013; Elsevier: Amsterdam, The Netherlands, 2013.
15. Mirolli, M.D. Kalina Cycle Power Systems in Waste Heat Recovery Applications. *Appl. Therm. Eng.* **2014**, *1–2*, 201–208.
16. Seckin, C. Effect of operational parameters on a novel combined cycle of ejector refrigeration cycle and Kalina cycle. *J. Energy Resour. Technol.* **2020**, *142*, 012001. [CrossRef]
17. Dostal, V.; Driscoll, M.J.; Hejzlar, P. *A Super Critical Carbon Dioxide Cycle for Next Generation Nuclear Reactors*; Massachusetts Institute of Technology, Center for Advanced Nuclear Energy Systems, Advanced Nuclear Power Program: Cambridge, MA, USA, 2004; 307p.
18. Weber, C.; Favrat, D. Conventional and advanced CO_2 based district energy systems. *Energy* **2010**, *35*, 5070–5081. [CrossRef]
19. Padilla, R.V.; Too, Y.C.S.; Benito, R.; Stein, W. Exergetic analysis of supercritical CO_2 Brayton cycles integrated with solar central receivers. *Appl. Energy* **2015**, *148*, 348–365. [CrossRef]
20. Hossain, M.; Chowdhury, J.I.; Balta-Ozkan, N.; Asfand, F.; Saadon, S.; Imran, M. Design Optimization of Supercritical Carbon Dioxide (s-CO_2) Cycles for Waste Heat Recovery From Marine Engines. *J. Energy Resour. Technol.* **2021**, *143*, 12120901. [CrossRef]
21. Korobitsyn, M. Industrial applications of the air bottoming cycle. *Energy Convers. Menag.* **2002**, *43*, 1311–1322. [CrossRef]
22. Czaja, D.; Chmielniak, T.; Lepszy, S. Selection of a gas turbine air bottoming cycle for Polish compressor stations. *J. Power Technol.* **2013**, *93*, 67–77.

23. Chmielniak, T.; Lepszy, S.; Czaja, D. The use of air bottoming cycle as a heat source for the carbon dioxide capture installation of a coal fired power unit. *Arch. Thermodyn.* **2011**, *32*, 89–101. [CrossRef]
24. Czaja, D.; Chmielniak, T.; Lepszy, S. Operation of a gas turbine air bottoming cycle at part load. *J. Power Technol.* **2013**, *93*, 279–286.
25. Ahmadi, A.; Jamali, D.H.; Ehyaei, M.A.; El Haj Assad, M. Energy, exergy, economic and exergo environmental analyses of gas and air bottoming cycles for production of electricity and hydrogen with gas reformer. *J. Clean. Prod.* **2020**, *259*, 120915. [CrossRef]
26. Parma, E.J.; Wright, S.A.; Vernon, M.E.; Fleming, D.D. *Supercritical CO$_2$ Direct Cycle Gas Fast Reactor (SC GFR) Concept*; 5285 Port Royal Rd. Springfield; U.S. Department of Commerce, National Technical Information Service: Albuquerque, NM, USA, 2011; Volume 22161, p. 54.
27. Pham, H.S.; Alpy, N.; Ferrasse, J.H.; Boutin, O.; Quenaut, J.; Tothill, M. Mapping of the thermodynamic performance of the supercritical CO$_2$ cycle and optimisation for a small modular reactor and a sodium-cooled fast reactor. *Energy* **2015**, *87*, 412–424. [CrossRef]
28. Bai, Z.; Zhang, G.; Yang, Y.; Wang, Z. Design performance simulation of a supercritical CO$_2$ cycle coupling with a steam cycle for gas turbine waste heat recovery. *J. Energy Resour. Technol.* **2019**, *141*, 102001. [CrossRef]
29. You, D.; Metghalchi, H. On the Supercritical Carbon Dioxide Recompression Cycle. *J. Energy Resour. Technol.* **2021**, *143*, 121701. [CrossRef]
30. Chen, Y. Thermodynamic Cycles using Carbon Dioxide as Working Fluid: CO$_2$ Transcritical Power Cycle Study. Ph.D. Thesis, School of Industrial Engineering and Management, Stockholm, Sweden, 2011; 128p.
31. Sanchez, D.; Chacartegui, R.; Jimenez-Espadafor, F.; Sanchez, T. A new concept for high temperature fuel cell hybrid systems using supercritical carbon dioxide. *J. Fuel Cell Sci. Technol.* **2009**, *6*, 021306. [CrossRef]
32. Turchi, C.S.; Ma, Z.; Neises, T.W.; Wagner, M.J. Thermodynamic study of advanced supercritical carbon dioxide power cycles for concentrating solar power systems. *J. Sol. Energy Eng* **2013**, *135*, 041007. [CrossRef]
33. Fang, L.; Li, Y.; Yang, X.; Yang, Z. Analyses of Thermal Performance of Solar Power Tower Station Based on a Supercritical CO$_2$ Brayton Cycle. *J. Energy Resour. Technol.* **2020**, *142*, 031301. [CrossRef]
34. Gequn, S.; Zhigang, Y.; Hua, T.; Peng, L.; Zhiqiang, X. Potential of the transcritical Rankine cycle using CO$_2$-based binary zeotropic mixtures for engine's waste heat recovery. *Energy Convers. Manag.* **2018**, *174*, 668–685.
35. Ayub, A.; Ahmed Sheikh, N.; Tariq, R.; Mahabat Khan, M.; Invermizzi, C.M. Exergetic optimization and comparison of combined gas turbine supercritical CO$_2$ power cycles. *J. Renew. Sustain. Energy* **2018**, *10*, 044703. [CrossRef]
36. Khadse, A.; Blanchette, L.; Kapat, J.; Vasu, S.; Hossain, J.; Donazzolo, A. Optimization of Supercritical CO$_2$ Brayton Cycle for Simple Cycle Gas Turbines Exhaust Heat Recovery Using Genetic Algorithm. *J. Energy Resour. Technol.* **2018**, *14*, 071601. [CrossRef]
37. Kim, M.S.; Ahn, Y.; Kim, B.; Lee, J.I. Study on the supercritical CO$_2$ power cycles for landfill gas firing gas turbine bottoming cycle. *Energy* **2016**, *111*, 893. [CrossRef]
38. Park, S.H.; Kim, J.Y.; Yoon, M.; Rhim, D.R.; Yeom, C. Thermodynamic and economic investigation of coal-fired power plant combined with various supercritical CO$_2$ Brayton power cycle. *Appl. Therm. Eng.* **2018**, *130*, 611–623. [CrossRef]
39. Sadatsakkak, S.A.; Ahmadi, M.H.; Ahmadi, M.A. Thermodynamic and thermo-economic analysis and optimization of an irreversible regenerative closed Brayton cycle. *Energy Convers. Manag.* **2015**, *94*, 124–129. [CrossRef]
40. Manikantachari KR, V.; Vasu, S.; Kapat, J. Effect of impurities on compressor and cooler in supercritical CO$_2$ cycles. *J. Energy Resour. Technol.* **2018**, *141*, 012003.
41. Stobart, R.K.; Wijewardane, A.; Allen, C. *The Potential for the Thermo-Electric Devices in Passenger Vehicle Applications*; SAE: Warrendale, PN, USA, 2010; p. 0833.
42. Cormos, C.C. Integrated assessment of IGCC power generation technology with carbon capture and storage (CCS). *Energy* **2012**, *42*, 434–445. [CrossRef]
43. Moullec, Y.L. Conceptual study of a high efficiency coal fired power plant with CO$_2$ capture using a supercritical CO$_2$ Brayton cycle. *Energy* **2013**, *49*, 32–46. [CrossRef]
44. Thatttai, A.T.; Oldenbroek, V.; Schoenmarkers, L.; Woudstra, T.; Aravind, P.V. Towards retrofitting integrated gasification combined cycle (IGCC) power plants with solid oxide fuel cells (SOFC) and CO$_2$ capture-a thermodynamic case study. *Appl. Therm. Eng.* **2017**, *114*, 170–185. [CrossRef]
45. Varga, Z.; Csaba, T. Techno-economic evaluation of waste heat recovery by organic Rankine cycle using pure light hydrocarbons and their mixtures as working fluid in a crude oil refinery. *Energy Convers. Manag.* **2018**, *174*, 793–801. [CrossRef]
46. Mignard, D. Correlating the chemical engineering plant cost index with macro-economic indicators. *Chem. Eng. Res. Des.* **2014**, *92*, 285–294. [CrossRef]
47. Ghazikhani, M.; Passandideh-Fard, M.; Mousavi, M. Two new high–performance cycles for gas turbine with air bottoming. *Energy* **2011**, *36*, 294–304. [CrossRef]